Mapping sites of interaction of p47–phox and flavocytochrome b with random-sequence peptide phage display libraries

Frank R. DeLeo*, Lixin Yu†, James B. Burritt*, Linda R. Loetterle†, Clifford W. Bond*, Algirdas J. Jesaitis*, and Mark T. Quinn†

Departments of †Veterinary Molecular Biology and *Microbiology, Montana State University, Bozeman, MT 59717

ABSTRACT   During assembly of the phagocyte NADPH oxidase, cytosolic p47-phox translocates to the plasma membrane and binds to flavocytochrome b, and binding domains for p47-phox have been identified on the C-terminal tails of both flavocytochrome b subunits. In the present report, we further examine the interaction of these two oxidase components by using random-sequence peptide phage display library analysis. Screening p47-phox with the peptide libraries identified five potential sites of interaction with flavocytochrome b, including three previously reported regions of interaction and two additional regions of interaction of p47-phox with gp91-phox and p22-phox. The additional sites were mapped to a domain on the first predicted cytosolic loop of gp91-phox encompassing residues $S^{86}TRVRRQL^{93}$ and to a domain near the cytosolic C-terminal tail of gp91-phox encompassing residues $F^{450}EWFADLL^{457}$. The mapping also confirmed a previously reported binding domain on gp91-phox ($E^{554}SGPRGVHFIF^{564}$) and putative Src homology 3 domain binding sites on p22-phox ($P^{156}PRPP^{160}$ and $G^{177}GPPGGP^{183}$). To demonstrate that the additional regions identified were biologically significant, peptides mimicking the gp91-phox sequences $F^{77}LRGSSACCSTRVRRQL^{93}$ and $E^{451}WFADLLQLLESQ^{463}$ were synthesized and assayed for their ability to inhibit NADPH oxidase activity. These peptides had EC_{50} values of 1 μM and 230 μM, respectively, and inhibited activation when added prior to assembly but did not affect activity of the preassembled oxidase. Our data demonstrate the usefulness of phage display library analysis for the identification of biologically relevant sites of protein–protein interaction and show that the binding of p47-phox to flavocytochrome b involves multiple binding sites along the C-terminal tails of both gp91- and p22-phox and other regions of gp91-phox nearer to the N terminus.

Stimulation of human neutrophils with a variety of agents induces these cells to generate microbicidal agents such as superoxide anion (O_2^-) and hydrogen peroxide (H_2O_2) (for review, see ref. 1). This response, which is commonly called the respiratory burst, results from the activation of a membrane-associated electron transport system, the NADPH oxidase (for review, see refs. 2 and 3). The importance of this system to host defense is exemplified by the severe recurrent infections experienced by individuals with chronic granulomatous disease (CGD), a hereditary disease resulting in defective NADPH oxidase activity (for review, see ref. 4). Phagocytes from individuals with CGD can ingest microorganisms normally; however, their inability to produce O_2^- and related microbicidal oxidants renders them ineffective at killing many pathogens (4).

Activation of the NADPH oxidase involves the interaction and/or assembly of several neutrophil components, some located on the plasma membrane and others in the cytosol (2,

3). The plasma-membrane-associated component directly implicated in the flow of electrons from NADPH to oxygen is a heterodimeric (5) flavocytochrome b (6, 7) that is composed of 91-kDa and 22-kDa subunits (known as gp91-phox and p22-phox, respectively). Three cytosolic proteins have also been shown to be absolutely required for NADPH oxidase activity. These proteins are p47-phox (8, 9), p67-phox (8, 9), and a second low molecular weight GTP-binding protein, Rac (10, 11). All three of these proteins are localized to the cytosol in unstimulated cells but translocate to the plasma membrane and become tightly associated with the membrane skeleton and/or other membrane-bound oxidase components upon cell activation (12, 13).

During NADPH oxidase assembly in the plasma membrane, p47-phox has been shown to interact directly with flavocytochrome b (14, 15), and p47-phox fails to translocate to the plasma membrane if flavocytochrome b is absent, e.g., in cells from patients with flavocytochrome b-deficient CGD (14, 16). In addition, in cells from patients with p47-phox-deficient CGD and in cell-free NADPH reconstitution assay systems, p67-phox fails to translocate in the absence of p47-phox (14, 17). Thus, the current model of NADPH oxidase assembly suggests that p47-phox plays a central role in assembly by binding directly to flavocytochrome b via specific peptide domains, and p67-phox binds indirectly or passively to the complex by virtue of its association with p47-phox (14, 18, 19).

Previous studies have shown that the C-terminal domains of p22- and gp91-phox interact with p47-phox during NADPH oxidase assembly. Kleinberg et al. (17) found that peptides corresponding to the C terminus of gp91-phox inhibited NADPH oxidase activity by blocking the interaction of p47-phox with flavocytochrome b. Nakanishi et al. (15) confirmed these studies and reported that the C-terminal region of p22-phox was also involved in the binding of p47-phox. Leusen et al. (20) found that a CGD missense mutation at residue 499 of gp91-phox resulted in nonfunctional flavocytochrome b and that a peptide encompassing this region blocked NADPH oxidase assembly. Finally, four groups (16, 18, 19, 21) have proposed that assembly of the NADPH oxidase also involved the interaction of multiple Src homology 3 (SH3) domains of cytosolic oxidase proteins with proline-rich targets in other oxidase components, including an interaction between the SH3 domain of p47-phox and a proline-rich region of p22-phox involving residues 149–162 ($K^{149}QPPSNPPPRPPAE^{162}$). Thus, it is clear that p47-phox interacts with flavocytochrome b at multiple sites or peptide domains on both subunits and that these interactions are essential for NADPH oxidase assembly.

To gain a further understanding of the interaction of p47-phox with flavocytochrome b and to identify other potential sites of binding between these important oxidase proteins, we screened recombinant p47-phox with random-sequence peptide phage display libraries to identify peptides that bound specifically to p47-phox and then compared these peptide

Abbreviations: CGD, chronic granulomatous disease; SH3, Src homology 3.

sequences to the sequences of gp91- and p22-phox. By using this procedure, we confirmed three previously reported (15–19, 21) regions of interaction of p47-phox with gp91- and p22-phox and identified two more sites of interaction of p47-phox with gp91-phox.

MATERIALS AND METHODS

Preparation and Fractionation of Neutrophils. Neutrophil membrane and cytosolic fractions were prepared from purified and cavitated human neutrophils (22) by sequential centrifugation (23).

Production and Purification of Recombinant p47-phox. Recombinant p47-phox was produced in recombinant baculovirus-infected Sf9 cells as described by Leto *et al.* (24). The purity (>99%) and identity of the recombinant p47-phox were confirmed by using SDS/PAGE and Western blot analysis with anti-p47-phox antibodies, and this protein was also found to be active in reconstituting NADPH oxidase activity in a cell-free NADPH oxidase assay system (data not shown).

Random-Sequence Peptide Library Screening. Random-sequence peptide bacteriophage library screening of recombinant p47-phox was performed by using biopanning with biotinylated p47-phox (25) and column screening. For the column screening, recombinant p47-phox was bound to CNBr-activated Sepharose 4B, the column was equilibrated with phage buffer (25), and 5 μl of a random-sequence hexapeptide fUSE5 bacteriophage library (26) or a nonapeptide-modified M13mp18 bacteriophage library (27) was incubated with the beads overnight at 4°C with gentle mixing. After washing the beads, bound phage were eluted with 0.1 M glycine (pH 2.2) and the eluate was neutralized. Eluted phage were amplified in K91 *Escherichia coli* cells on solid LB agar (28) or in liquid culture, extracted (28), and reapplied two more times to the p47-phox column. The third eluate was plated with K91 cells on LB plates containing kanamycin at 100 μg/ml (nonapeptide library) or tetracycline at 40 μg/ml (hexapeptide library). Random colonies were picked and sequenced by using a gene III-specific primer (28).

Cell-Free NADPH Oxidase Assay. Cell-free NADPH oxidase activity was measured as described by Yu *et al.* (29). The reaction mixture [50 μM cytochrome c/10 μM FAD/1 mM EGTA/2 mM NaN$_3$/10 μM guanosine 5'-[γ-thio]triphosphate/10–20 ng of membrane protein/20–40 ng of cytosol/ with or without superoxide dismutase (45 μg/ml)/assay buffer (10 mM potassium phosphate/130 mM NaCl, pH 6.7) in 1 ml] was incubated for 2 min at 25°C and then 100 μM SDS was added. After 3 min, 200 μM NADPH was added to initiate the reaction, and the rate of O$_2^-$ production was measured continuously at 550 nm. To analyze peptide inhibition, peptides dissolved in assay buffer were added to the reaction mixture before and after SDS addition (the peptides used were >95% pure, and their sequences were confirmed by MS).

RESULTS

Identification of p47-phox Binding Regions on Flavocytochrome b_{558}. To identify regions of interaction between p47-phox and flavocytochrome b, p47-phox columns and streptavidin-biotin-linked p47-phox biopans were used to affinity-select bacteriophage from hexapeptide and nonapeptide libraries. The random-region sequences from 128 isolated bacteriophage were screened to yield four peptide consensus sequence motifs (Table 1). Twenty-three of the phage peptides contained sequences similar to gp91-phox residues 86–90 (S^{86}TRVRRQL^{93}) located in the first predicted cytosolic loop [based on hydropathy analysis (30)] of gp91-phox. As shown in Table 1, one of the isolates contained a 5-residue match within this region of gp91-phox, and two isolated phage peptide sequences contained 4 residues

Table 1. p47-phox-binding phage displaying sequences of homology with flavocytochrome b

gp91-phox			gp22-phox
S^{85}TRVRRQL^{93}	F^{450}EWFADLL^{457}	E^{554}SGPRGVHFIF^{564}	G^{177}GPPGG^{182}/ P^{156}PRPP^{160}
STRVRWGAY	VRHDLLF	SSGPWKEHF	GGPPRV
ATRVPRKHW	ALRDLLYPD	MFSPWNDHF	FTKKIYGPP
TRVMRE	KFDLLSPFS	MFSPWNDHF	YLDGGP
TRPRWHKHA	LGDLLKDMY	MFSPWNDHF	HGMKFPGPA
RVRQFG	WHDLGF	ESGAFA	TQQRGP
VRHDLLF	WDFSDLHW	FRIGHF	LMVKPRKHW
RVRQFG	DLTRQG	GSHFSIFS	KWHKNHPP
KRHRRKTWG	DVSWDLITA	SSVHYM	FTWPRW
LRVWNL	AARVDPLVK	SSVHYM	AHKHWRPRT
WHKHWTRPV	VPARFDLDN	PALPWAEHF	
WHKTWRVKG	PGGDLY	KGAPWQEHF	
VRPARHWWK	TFDLTS	KGAPWQEHF	
VRPARHWWK		VHIMKL	
KVLPDVRAA		PWSEHF	
VRAVTL			
VRPPGG			
SAVRIL			
ARLAVR			
ARSPRQIHI			
ILRQAN			
DLTRQG			
NRHIRRL			
VYGGSRQWG			

Phage recovered from three screening experiments were sequenced and the four flavocytochrome b consensus motifs were aligned. Residues identical to the corresponding flavocytochrome b sequences are underlined, residues shifted in position are in italic type, and conservative substitutions are in boldface type.

identical with S^{86}TRVRRQL^{93}. Twenty other phage clones contained 2- and 3-residue matches to this region of gp91-phox (see Table 1). Additionally, the presence of conservative substitutions and/or 1-residue shifts in these bacteriophage sequences compared to the gp91-phox sequence suggests an even greater similarity of many of the phage peptides to this region (see Table 1). Interestingly, 3 phage supporting this consensus sequence also had homology to a region encompassing residues 89–94 of p22-phox [proposed to be extracellular (30)]; however, no other phage sequences supported this region as a dominant consensus motif. It should be emphasized that the regions mapped by phage display library analysis represent consensus sequences supported by a number of different phage clones. Each of these phage sequences alone, especially those contributing only 2-residue matches to the consensus sequence, could potentially map to several regions in the same protein. However, in the context of a consensus sequence supported by multiple phage peptides and independent biochemical or immunological evidence, 2-residue matches provide important supporting data (26, 31).

In addition to the identification of a consensus sequence mapping to gp91-phox residues 86–90, three other areas of interaction with flavocytochrome b were identified by consensus sequence analysis among the selected phage. One of these motifs mapped to a region of gp91-phox encompassing F^{450}EWFADLL^{457} and was represented by 12 of the bacteriophage sequences (see Table 1). Five of these phage contained 3-residue matches within this region of gp91-phox, and several of these phage sequences also contained a phenylalanine that could possibly represent Phe^{450} and/or Phe^{453} if either residue was juxtaposed near D^{455}LL^{457} in the tertiary structure. The remaining seven bacteriophage sequences displayed 2- and possibly 3- (based on conservative substitutions and/or one residue shifts) residue matches supporting the overall consensus motif. The smaller number of phage displaying this motif (as compared to the STRVRRQL motif) may be an indication of a lower-affinity interaction of p47-phox (or of the phage peptides) with gp91-phox at this site, and peptide inhibition studies described below support this idea. It is possible that phage displaying the DLL motif may also be representative of

a p47-phox–p47-phox interactive site at p47-phox residues L[259]LD[261] and/or L[114]LD[116].

Nine bacteriophage with random regions displaying similarity to residues 158–162 and 177–183 of p22-phox (P[156]PRPP[160] and G[177]GPPGGP[183]) were also selected by phage display library screening (see Table 1). One of these clones had a 4-residue match to G[177]GPPGGP[183] of p22-phox and also a 3-residue match to P[156]PRPP[160] of p22-phox. Eight other clones had 2- and 3-residue matches, supporting the consensus motifs mapped to these regions of p22-phox. It is interesting that both of these regions are located within proline-rich domains of p22-phox and represent putative p47-phox SH3 domain binding motifs (16, 18, 19).

Finally, bacteriophage representative of a C-terminal region of gp91-phox (E[554]SGPRGVHFIF[564]) were also identified by phage display library screening (Table 1), and ≈15 of the isolated phage displayed random peptides similar to this domain. One of these phage peptides had 5 identical residues, two others displayed 4-residue matches, and the remaining phage contained 2- and 3-residue matches to this region of gp91-phox. In addition, the possibility of conservative substitutions and 1-residue shifts in these sequences would make the fit even stronger. This region of gp91-phox has been identified as a site of interaction with p47-phox (15, 17), and therefore, identification of phage peptides mapped to this domain and to the p22-phox proline-rich domains described above confirms previous results indicating that these are p47-phox binding regions (15–19) and demonstrates that random-sequence peptide phage display library analysis is a valid sensitive method for identifying biologically relevant sites of protein–protein binding interaction.

Peptide Inhibition Assays. To determine whether the regions selected by the random-sequence peptide library analysis were functionally significant, peptides matching residues 77–93 and 451–463 of gp91-phox (i.e., F[77]LRGSSACCSTRVRRQL[93] and E[451]WFADLLQLLESQ[463], respectively) and a peptide matching residues 176–195 of p22-phox (A[176]GGPPGGPQVNPIP-VTDEVV[195]) were synthesized and assayed for their ability to alter NADPH oxidase activity in a cell-free NADPH oxidase assay system. As shown in Fig. 1, F[77]LRGSSACCSTRVRRQL[93] and E[451]WFADLLQLLESQ[463] specifically inhibited NADPH oxidase activity with an EC_{50} of 1 and 230 μM, respectively, but a control inactive peptide had no effect over the concentration ranges tested. The p22-phox peptide A[176]GGPPGGPQVN-PIPVTDEVV[195] also inhibited NADPH oxidase activity but was much less effective than the gp91-phox peptides (EC_{50} ≈500 μM; data not shown). It is not clear why this peptide was not as active in our system compared to Nakanishi *et al.* (15); however, these differences may be attributed, in part, to differences in our assay systems. The phage peptides mapping to this region of p22-phox were also similar to a second proline-rich region of p22-phox, encompassing K[149]QPPSNPPPRPPAE[162]. Thus, it is possible that the high-affinity binding domain represented by these phage is actually located within p22-phox residues 149–162 and that residues 176–195 of p22-phox represent a lower-affinity binding region for p47-phox that does not involve SH3 domain interactions. In support of this possibility, Leto *et al.* (19) found that the p22-phox peptide A[176]GGPPGGPQVNPIPVTDEVV[195] was not able to block binding of p47-phox SH3 domains to p22-phox, whereas the p22-phox peptide K[149]QPPSNPPPRPPAE[162] did.

To determine the active region of the most inhibitory peptide (F[77]LRGSSACCSTRVRRQL[93]), each half of this peptide was synthesized and tested for inhibitory activity. While the C-terminal half of the peptide (C[85]STRVRRQL[93]) inhibited oxidase activity in the cell-free assay system with a similar efficacy as the full-length peptide (EC_{50} ≈3 μM), the N-terminal half (F[77]LRGSSACC[85]) was inactive up to 500 μM (Fig. 2). These results establish that the active half of the peptide contains the peptide motif identified by phage library analysis (STRVRRQL), and this represents a high-affinity
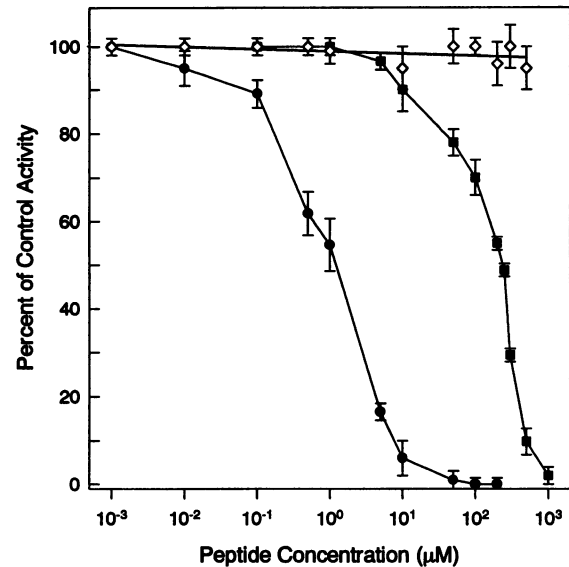
FIG. 1. Effect of phage-mapped flavocytochrome *b* peptides on NADPH oxidase activity. Peptides F[77]LRGSSACCSTRVRRQL[93] (●), E[451]WFADLLQLLESQ[463] (■), and control peptide KLSYR-PRDSNE (◇) were added to the cell-free NADPH oxidase assay system, and O_2^- generation was measured. The results are expressed as percent of control activity [457 ± 18 nmol of O_2^- per min per mg of membrane protein (mean ± SD; n = 3)] and represent the mean ± SD of three experiments.

binding site for p47-phox, while gp91-phox residues represented by the N-terminal half of the peptide (residues 77–93) are probably not involved in this binding interaction.

To evaluate whether the inhibitory peptides were blocking assembly or inhibiting activity of the assembled oxidase, we analyzed the ability of these peptides to inhibit activity before and after SDS addition. As shown in Table 2, all of the active peptides inhibited activity when added prior to SDS addition but failed to inhibit oxidase activity when added ≥3 min after SDS (i.e., after complete oxidase assembly), suggesting that the regions of flavocytochrome *b* represented by these peptides participate in the binding of p47-phox and are necessary for correct assembly of the NADPH oxidase. After assembly, these sites and the complementary binding sites on p47-phox then become inaccessible to peptides. This would explain the inability of these peptides to inhibit the production of O_2^- if they are added after oxidase assembly. However, peptides added with the SDS and up to 3 min after SDS addition showed a time-dependent increase in inhibitory activity with full activity occurring at ≥3 min after SDS addition (see Table 2). This observation is consistent with that of Kleinberg *et al.* (17) who found that oxidase assembly in the cell-free assay system exhibited a variable lag time between addition of arachidonic acid and full oxidase assembly. Thus, prior to complete assembly of the NADPH oxidase (i.e., at times ≤3 min), inhibitory peptides still have the ability to block assembly of unassembled and/or unstable NADPH oxidase complexes.

DISCUSSION

The binding of p47-phox to flavocytochrome *b* plays a key role in assembly of the neutrophil NADPH oxidase, and agents that interfere with this interaction can completely block assembly and activation of this important host defense system (15, 17–19). Previous studies on the interaction of p47-phox with flavocytochrome *b* have identified several sites of binding between these two oxidase components; however, all of these sites have been localized either to the C-terminal region of gp91-phox (≈last 80 residues) or in two proline-rich domains
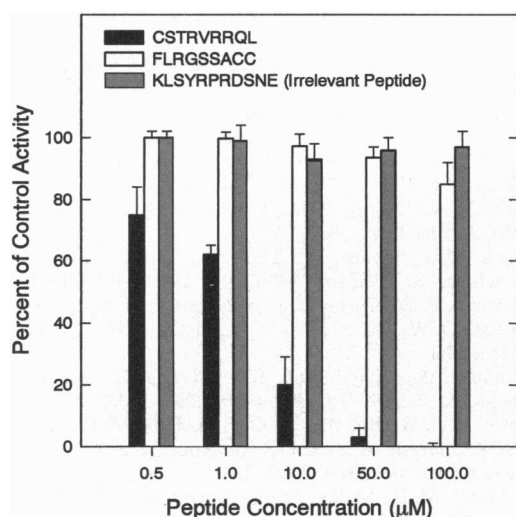
FIG. 2. Determining the active region of gp91-phox peptide F^{77}LRGSSACCSTRVRRQL^{93}. Peptides were added to the cell-free NADPH oxidase assay system, and O_2^- generation was measured. The results are expressed as percent of control activity [336 ± 28 nmol of O_2^- per min per mg of membrane protein (mean ± SD; $n = 6$)] and represent the mean ± SD of three experiments.

on the C-terminal half of p22-phox (Fig. 3). Two of the binding domains for p47-phox on flavocytochrome b were identified because they encompassed sites of CGD mutations and/or putative SH3 domain binding motifs (16, 18–20); the others were identified by screening flavocytochrome b cytoplasmic regions with synthetic peptides (15, 17). These approaches are limited, however, because some sites of interaction of these proteins may not be represented by genetic mutations and/or well-defined structural motifs. Therefore, we have utilized another approach to identify sites of interaction between p47-phox and flavocytochrome b based on the use of random-sequence peptide phage display library analysis to map p47-phox binding domains on flavocytochrome b. Random-sequence peptide phage display analysis has been used to identify antibody epitopes (26, 32), receptor ligands (33–36), protease substrates (37), and protein structural epitopes (31,

Table 2. Analysis of the inhibitory activity of flavocytochrome b peptides added before and after assembly of the NADPH oxidase

Sample	Time, min	% of control activity
Control	—	100
+ F^{77}LRGSSACCSTRVRRQL^{93} (10 μM)	−3	9 ± 5
+ F^{77}LRGSSACCSTRVRRQL^{93} (10 μM)	−2	20 ± 4
+ F^{77}LRGSSACCSTRVRRQL^{93} (10 μM)	−1	15 ± 5
+ F^{77}LRGSSACCSTRVRRQL^{93} (10 μM)	0	24 ± 7
+ F^{77}LRGSSACCSTRVRRQL^{93} (10 μM)	+1/2	52 ± 1
+ F^{77}LRGSSACCSTRVRRQL^{93} (10 μM)	+1	65 ± 2
+ F^{77}LRGSSACCSTRVRRQL^{93} (10 μM)	+2	73 ± 3
+ F^{77}LRGSSACCSTRVRRQL^{93} (10 μM)	+3	96 ± 2
+ F^{77}LRGSSACC^{85} (10 μM)	−3	98 ± 4
+ F^{77}LRGSSACC^{85} (10 μM)	+3	98 ± 2
+ C^{85}STRVRRQL^{93} (10 μM)	−3	21 ± 4
+ C^{85}STRVRRQL^{93} (10 μM)	+3	97 ± 2
+ E^{451}WFADLLQLLESQ^{463} (250 μM)	−3	54 ± 6
+ E^{451}WFADLLQLLESQ^{463} (250 μM)	+3	98 ± 2

Peptides were added at the indicated time points before (+) and after (−) addition of SDS to the cell-free assay system, and the results are reported as percent of control activity [306 ± 10 nmol of O_2^- per min per mg of membrane protein (mean ± SD; $n = 5$)]. The results are expressed as mean ± SD of three experiments.

38); we have used (27) it to determine flavocytochrome b monoclonal antibody epitopes.

The interaction of p47-phox with gp91-phox appears to be highly complex with multiple sites of interaction. p47-phox is ≈80% of the molecular weight of the gp91-phox core protein, making it probable that p47-phox interacts with gp91-phox at multiple sites to form a highly stable complex. Previously, two sites of interaction of these proteins along the C-terminal tail of gp91-phox were found by using peptide screening and genetic analysis of a CGD mutation, respectively (17, 20). Our data demonstrate two additional binding sites between these proteins (see Fig. 3), including a very high-affinity binding site in the region of the first predicted cytosolic loop of gp91-phox, and confirmation of the phage library screening with peptide inhibition studies indicates that this region (gp91-phox residues 86–93) represents one of the highest affinity interactions of these two proteins reported. This finding suggests that the interaction of p47-phox with gp91-phox involves more of the gp91-phox molecule than just the C-terminal tail (although three potential binding sites are present in this region). This multivalent binding interaction and possible sequestering of p47-phox within the flavocytochrome b heterodimer could then explain why peptides added after NADPH oxidase assembly have no effect on oxidase activity and fail to disrupt the assembled oxidase complex (17).

The p47-phox binding domain mapped to gp91-phox residues 85–93 contains three basic amino acids, suggesting that electrostatic interactions may contribute to the binding process. Previously, Joseph *et al.* (39) reported that any polybasic peptide (≥5 basic residues) could inhibit NADPH oxidase activity; however, they also found that an 11-residue peptide
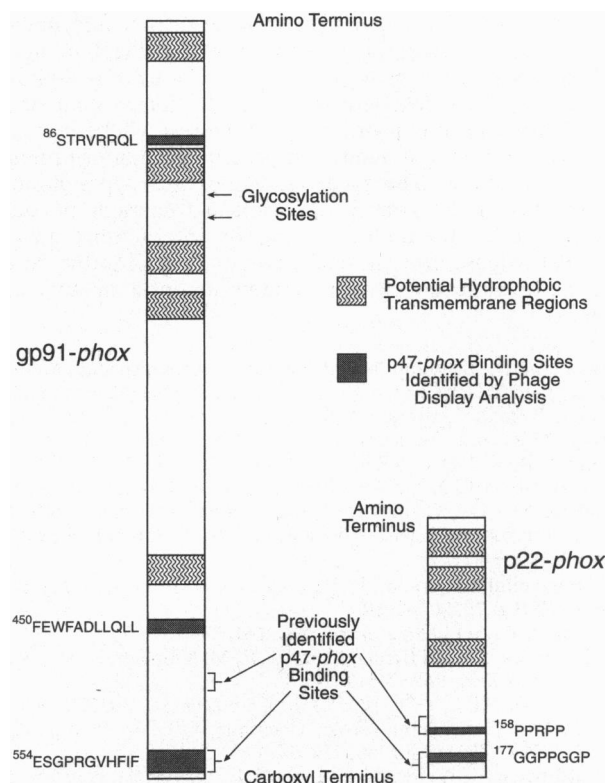
FIG. 3. Extended model of gp91-phox and p22-phox illustrating p47-phox binding sites. This model shows all currently known sites of interaction of p47-phox with flavocytochrome b. Sites identified by phage display analysis are indicated as shaded regions, and the respective sequences are shown. The N termini of both subunits are proposed to be extracellular, and the C termini have been shown to be cytosolic. The predicted transmembrane regions shown are based on hydropathy analyses (30).

containing 6 lysines had no effect on oxidase activity. We have analyzed a number of polybasic peptides that have no inhibitory effect on NADPH oxidase activity, including our control peptide, which contains three basic residues. Nauseef *et al.* (40) reported that several polybasic peptides (HQRSRKRLSQD, PPRRSSIRNA, and RRNSVR) failed to inhibit NADPH oxidase activity in a cell-free system (note the similarity between their inactive peptide RRNSVR and our most active peptide CSTRVRRQL), and we have recently confirmed these results with similar peptides (data not shown). Thus, the inhibition of NADPH oxidase activity by gp91-phox peptides F[77]LRGSSACCSTRVRRQL[93] and C[85]STRVRRQL[93] is specific to these sequences and/or the charge distribution represented by these sequences. Therefore, we suggest that the apparent nonspecific inhibition of oxidase activity by polybasic peptides, as suggested by Joseph *et al.* (39), may really be due to the blocking of specific binding interactions (in this case between p47-phox and gp91-phox) that involve basic amino acid-enriched domains on one or both of the interacting proteins (in this case on gp91-phox).

The C-terminal half of p22-phox has been implicated in NADPH oxidase assembly via proline-rich SH3 domain binding sites. Sumimoto *et al.* (18) and Leto *et al.* (19) reported that p47-phox SH3 domains interacted with a proline-rich SH3-binding region of p22-phox encompassing residues K[149]QPPSNPPPRPPAE[162], and our results support their findings (Fig. 3). Sparks *et al.* (35) and Cheadle *et al.* (36) reported the identification of SH3 domain binding peptides affinity-selected by random-sequence peptide phage display library analysis of SH3 domain fusion proteins. Our identification of putative SH3 binding domain(s) on p22-phox by phage display analysis is consistent with these findings and extends this approach to the screening of an intact biologically active protein. In addition, our results provide further information establishing the essential core motif(s) for the binding of p47-phox SH3 domains to proline-rich regions of p22-phox.

The use of random-sequence peptide library analysis to directly screen proteins or ligands of interest will be useful in the identification of a number of protein–protein or protein–ligand interactions. The understanding of these types of interactions has implications in the clinical treatment of many diseases, and the understanding of interactions among NADPH oxidase proteins could eventually lead to the development of more effective treatments for inflammatory diseases.

1. Baggiolini, M., Boulay, F., Badwey, J. A. & Curnutte, J. T. (1993) *FASEB J.* 7, 1004–1010.
2. Clark, R. A. (1990) *J. Infect. Dis.* 161, 1140–1147.
3. Chanock, S. J., El Benna, J., Smith, R. M. & Babior, B. M. (1994) *J. Biol. Chem.* 269, 24519–24522.
4. Dinauer, M. C. (1993) *Crit. Rev. Clin. Lab. Sci.* 30, 329–369.
5. Parkos, C. A., Allen, R. A., Cochrane, C. G. & Jesaitis, A. J. (1987) *J. Clin. Invest.* 80, 732–742.
6. Rotrosen, D., Yeung, C. L., Leto, T. L., Malech, H. L. & Kwong, C. H. (1992) *Science* 256, 1459–1462.
7. Segal, A. W., West, I., Wientjes, F., Nugent, J. H. A., Chavan, A. J., Haley, B., Garcia, R. C., Rosen, H. & Scarce, G. (1992) *Biochem. J.* 284, 781–788.
8. Volpp, B. D., Nauseef, W. M. & Clark, R. A. (1988) *Science* 242, 1295–1297.
9. Nunoi, H., Rotrosen, D., Gallin, J. I. & Malech, H. L. (1988) *Science* 242, 1298–1301.
10. Knaus, U. G., Heyworth, P. G., Evans, T., Curnutte, J. T. & Bokoch, G. M. (1991) *Science* 254, 1512–1515.
11. Abo, A., Pick, E., Hall, A., Totty, N., Teahan, C. G. & Segal, A. W. (1991) *Nature (London)* 353, 668–670.
12. Clark, R. A., Volpp, B. D., Leidal, K. G. & Nauseef, W. M. (1990) *J. Clin. Invest.* 85, 714–721.
13. Quinn, M. T., Evans, T., Loetterle, L. R., Jesaitis, A. J. & Bokoch, G. M. (1993) *J. Biol. Chem.* 268, 20983–20987.
14. Heyworth, P. G., Curnutte, J. T., Nauseef, W. M., Volpp, B. D., Pearson, D. W., Rosen, H. & Clark, R. A. (1991) *J. Clin. Invest.* 87, 352–356.
15. Nakanishi, A., Imajohohmi, S., Fujinawa, T., Kikuchi, H. & Kanegasaki, S. (1992) *J. Biol. Chem.* 267, 19072–19074.
16. Leusen, J. H. W., Bolscher, B. G. J. M., Hilarius, P. M., Weening, R. S., Kaulfersch, W., Seger, R. A., Roos, D. & Verhoeven, A. J. (1994) *J. Exp. Med.* 180, 2329–2334.
17. Kleinberg, M. E., Malech, H. L. & Rotrosen, D. (1990) *J. Biol. Chem.* 265, 15577–15583.
18. Sumimoto, H., Kage, Y., Nunoi, H., Sasaki, H., Nose, T., Fukumaki, Y., Ohno, M., Minakami, S. & Takeshige, K. (1994) *Proc. Natl. Acad. Sci. USA* 91, 5345–5349.
19. Leto, T. L., Adams, A. G. & de Mendez, I. (1994) *Proc. Natl. Acad. Sci. USA* 91, 10650–10654.
20. Leusen, J. H. W., De Boer, M., Bolscher, B. G. J. M., Hilarius, P. M., Weening, R. S., Ochs, H. D., Roos, D. & Verhoeven, A. J. (1994) *J. Clin. Invest.* 93, 2120–2126.
21. Finan, P., Shimizu, Y., Gout, I., Hsuan, J., Truong, O., Butcher, C., Bennett, P., Waterfield, M. D. & Kellie, S. (1994) *J. Biol. Chem.* 269, 13752–13755.
22. Quinn, M. T., Parkos, C. A. & Jesaitis, A. J. (1989) *Biochim. Biophys. Acta* 987, 83–94.
23. Fujita, I., Takeshige, K. & Minakami, S. (1987) *Biochim. Biophys. Acta* 931, 41–48.
24. Leto, T. L., Garrett, M. C., Fujii, H. & Nunoi, H. (1991) *J. Biol. Chem.* 266, 19812–19818.
25. Smith, G. P. & Scott, J. K. (1993) *Methods Enzymol.* 217, 228–257.
26. Scott, J. K. & Smith, G. P. (1990) *Science* 249, 386–390.
27. Burritt, J. B., Quinn, M. T., Jutila, M. A., Bond, C. W. & Jesaitis, A. J. (1995) *J. Biol. Chem.* 270, 1–8.
28. Sambrook, J., Fritsch, E. F. & Maniatis, T. (1989) *Molecular Cloning: A Laboratory Manual* (Cold Spring Harbor Lab. Press, Plainview, NY).
29. Yu, L., Takeshige, K., Nunoi, H. & Minakami, S. (1993) *Biochim. Biophys. Acta Mol. Cell Res.* 1178, 73–80.
30. Parkos, C. A., Quinn, M. T., Sheets, S. & Jesaitis, A. J. (1992) in *Molecular Basis of Oxidative Damage by Leukocytes*, eds. Jesaitis, A. J. & Dratz, E. A. (CRC, Boca Raton, FL), pp. 45–56.
31. Devlin, J. J., Panganiban, L. C. & Devlin, P. E. (1990) *Science* 249, 404–406.
32. Cwirla, S. E., Peters, E. A., Barrett, R. W. & Dower, W. J. (1990) *Proc. Natl. Acad. Sci. USA* 87, 6378–6382.
33. Yayon, A., Aviezer, D., Safran, M., Gross, J. L., Heldman, Y., Cabilly, S., Givol, D. & Katchalski-Katzir, E. (1993) *Proc. Natl. Acad. Sci. USA* 90, 10643–10647.
34. Koivunen, E., Wang, B. & Ruoslahti, E. (1994) *J. Cell Biol.* 124, 373–380.
35. Sparks, A. B., Quilliam, L. A., Thorn, J. M., Der, C. J. & Kay, B. K. (1994) *J. Biol. Chem.* 269, 23853–23856.
36. Cheadle, C., Ivashchenko, Y., South, V., Searfoss, G. H., French, S., Howk, R., Ricca, G. A. & Jaye, M. (1994) *J. Biol. Chem.* 269, 24034–24039.
37. Matthews, D. J. & Wells, J. A. (1993) *Science* 260, 1113–1117.
38. Hoess, R. H., Mack, A. J., Walton, H. & Reilly, T. M. (1994) *J. Immunol.* 153, 724–729.
39. Joseph, G., Gorzalczany, Y., Koshkin, V. & Pick, E. (1994) *J. Biol. Chem.* 269, 29024–29031.
40. Nauseef, W. M., McCormick, S., Renee, J., Leidal, K. G. & Clark, R. A. (1993) *J. Biol. Chem.* 268, 23646–23651.